Redox Biology 20 (2019) 285–295

Contents lists available at ScienceDirect

Redox Biology

journal homepage: www.elsevier.com/locate/redox

Research Paper

Calcium signals between the ryanodine receptor- and mitochondria critically regulate the effects of arsenite on mitochondrial superoxide formation and on the ensuing survival *vs* apoptotic signaling

Andrea Guidarelli, Mara Fiorani, Liana Cerioni, Orazio Cantoni*

Department of Biomolecular Sciences, University of Urbino, Carlo Bo, via Saffi 2, 61029 Urbino, PU, Italy

ARTICLE INFO

Keywords:
Arsenite
Ryanodine receptor
Inositol-1, 4, 5-triphosphate receptor
Mitochondrial Ca^{2+}
Mitochondrial superoxide
Survival *vs* apoptotic signaling

ABSTRACT

A low concentration of arsenite (6 h), selectively stimulating the intraluminal crosstalk between the inositol-1, 4, 5-triphosphate receptor and the ryanodine receptor (RyR), increased the mitochondrial transport of RyR-derived Ca^{2+} through the mitochondrial Ca^{2+} uniporter. This event was characterized in intact and permeabilized cells, and was shown to be critical for mitochondrial superoxide ($mitoO_2^{\cdot-}$) formation. Inhibition of mitochondrial Ca^{2+} accumulation therefore prevented the effects of arsenite, in both the mitochondrial (e.g., cardiolipin oxidation) and extramitochondrial (e.g., DNA single- strand breakage) compartments, and suppressed the Nrf2/GSH survival signaling. The effects of arsenite on Ca^{2+} homeostasis and $mitoO_2^{\cdot-}$ formation were reversible, as determined after an additional 10 h incubation in fresh culture medium and by measuring long-term viability. A 16 h continuous exposure to arsenite instead produced a sustained increase in the cytosolic and mitochondrial Ca^{2+} concentrations, a further increased $mitoO_2^{\cdot-}$ formation and mitochondrial permeability transition. These events, followed by delayed apoptosis (48 h), were sensitive to treatments/manipulations preventing mitochondrial Ca^{2+} accumulation. Interestingly, cells remained viable under conditions in which the deregulated Ca^{2+} homeostasis was not accompanied by $mitoO_2^{\cdot-}$ formation.

In conclusion, we report that the fraction of Ca^{2+} taken up by the mitochondria in response to arsenite derives from the RyR. Mitochondrial Ca^{2+} appears critical for $mitoO_2^{\cdot-}$ formation and for the triggering of both the cytoprotective and apoptotic signaling. The effects of arsenite were reversible, whereas its prolonged exposure caused a sustained increase in mitochondrial Ca^{2+} and $mitoO_2^{\cdot-}$ formation, and the prevalence of the apoptotic *vs* survival signaling.

1. Introduction

It is well established that reactive oxygen species (ROS) can be generated in multiple compartments and by different sources, which include the respiratory chain, a large family of NADPH oxidases, lipoxygenases, uncoupled nitric oxide synthase, xanthine oxidase, etc. [1–4]. These diverse conditions are expected to result in different local concentrations of H_2O_2, depending on the site in which superoxide ($O_2^{\cdot-}$) formation takes place and its dismutation to H_2O_2 ensues. Furthermore, ROS released by one source can eventually recruit other mechanisms leading to enhanced ROS release [5,6]. There is for example the possibility that activation of NADPH oxidase results in enhanced H_2O_2 formation and in H_2O_2-dependent mitochondrial dysfunction, which in turn leads to additional ROS release [7,8].

The complexity of these events is further increased by the interplay between the mechanisms involved in ROS release and Ca^{2+} mobilization, for at least three separate reasons. The first one is related to the fact that most of the mechanisms mediating ROS formation, in particular those based on inhibition of electron transport in the respiratory chain, or on NADPH oxidase activation, are Ca^{2+}-dependent [6,9]. The

Abbreviation: AA, ascorbic acid; 2-APB, 2-aminoethoxydiphenyl borate; Cf, caffeine; 7-chloro-5–2-chlorophenyl-1,5-dihydro-4,1-benzothiazepin-23H-one, CGP-37157; CsA, cyclosporin A; DHR, dihydrorhodamine 123; D-cells, differentiated cells; $[Ca^{2+}]_c$, cytosolic Ca^{2+} concentration; $[Ca^{2+}]_m$, mitochondrial Ca^{2+} concentration; GSH, glutathione; IP_3R, inositol 1,4,5-trisphosphate receptor; mNCX, mitochondrial Na^+/Ca^{2+} exchanger; $mitoO_2^{\cdot-}$, mitochondrial superoxide; MCU, mitochondrial Ca^{2+} uniporter; MPT, mitochondrial permeability transition; NAO, 10-N-nonyl acridine orange; Nrf2, nuclear factor erythroid 2 p45-related factor 2; RD-cells, respiration-deficient cells; RP-cells, respiration-proficient cells; Ry, ryanodine; RyR, ryanodine receptor; ROS, reactive oxygen species; RR, ruthenium red

* Correspondence to: Dipartimento di Scienze Biomolecolari, Sezione di Farmacologia e Farmacognosia, Università degli Studi di Urbino, Via S. Chiara 27, 61029 Urbino, PU, Italy.

E-mail address: orazio.cantoni@uniurb.it (O. Cantoni).

https://doi.org/10.1016/j.redox.2018.10.015
Received 7 August 2018; Received in revised form 11 October 2018; Accepted 19 October 2018
Available online 23 October 2018

second reason is that ROS may effectively stimulate the release of Ca^{2+} from both the inositol-1, 4, 5-triphosphate receptor (IP_3R) or ryanodine receptor (RyR) [9–11]. The third one is instead that Ca^{2+} stimulates the activity of nitric oxide synthase, thereby resulting in the formation of reactive nitrogen species, as peroxynitrite [12,13], which effectively alter Ca^{2+} homeostasis [13], or eventually lead to further $O_2^{\cdot-}/H_2O_2$ formation [12–14].

These general principles make the point that the issues of where ROS and Ca^{2+} are released, and how these events are interconnected, are difficult to address, and should therefore involve carefully planned experiments, using appropriate and possibly simplified approaches. For example, the cell type should be carefully selected since different cells may differentially express specific ROS sources and/or Ca^{2+} channels. The concentration of the agent under investigation should also be carefully chosen since toxicity and ATP depletion burst most of the above complicating factors [5,9,11].

Trivalent arsenic, a widely distributed environmental toxic metalloid and human carcinogen [15–17], that produces deleterious effects in diverse biomolecules located in different subcellular compartments [16,17], represents a prototype of an agent promoting events characterized by the above complexities. Furthermore, arsenite presents an additional complication related to its ability to bind to thiol residues in proteins [16,18], which may on the one hand directly result in ROS formation and on the other hand directly deregulate Ca^{2+} homeostasis, since the endoplasmic reticulum presents critical cysteines in both the IP_3R and RyR [10,19]. Not surprisingly, different studies using different cell types and arsenite concentrations reported evidence of ROS formation from different sources [16,17] and Ca^{2+} mobilization through different mechanisms [20–23], with the interplay between these events rarely determined [20,23].

Understanding the details of the above effects mediated by arsenite is of critical importance since the interplay between Ca^{2+} and ROS is central to the regulation of events leading to the induction of skin, liver, lung, urinary tract and bladder cancers [15–17] as well as cardiovascular, hepatic, renal and nervous system disorders [16,17]. Exposure to arsenic has a major impact on human health, as over 200 million people are exposed to arsenic, in particular through drinking water [15].

With these considerations in mind, we initially selected a cell type, U937 cells, in which a low concentration of arsenite exclusively promotes mitochondrial $O_2^{\cdot-}$ ($mitoO_2^{\cdot-}$) formation [24–27], to then address specific questions on the effect mediated by the metalloid on Ca^{2+} homeostasis [28]. It should be also mentioned that this cell line presents the following advantages: i) it expresses functional high affinity Na^+ dependent vitamin c transporter 2 in both the plasma and mitochondrial membranes, thereby allowing the accumulation of high and low amounts of ascorbic acid (AA) in mitochondria and in the cytosol, respectively [29–31]. Mitochondrial AA can then be functional for an effective and selective scavenging of $mitoO_2^{\cdot-}$. ii) this cell line does not express constitutive nitric oxide synthase and fails to express the inducible isoform in response to arsenite [24,26,27]. We can therefore rule out the involvement of peroxynitrite in our experiments, and hence simplify the interpretation of their outcomes; iii) this cell line can be easily manipulated to induce mitochondrial respiratory deficiency [25,26]. iv) these cells express both the IP_3R and the RyR [28,32–34]. v) these cells can be easily differentiated to monocytes with down-regulated RyR expression [34].

We recently investigated the effects of a low concentration (2.5 μM) of arsenite (6 h) using the parental U937 cell line, from now on referred to as respiration-proficient RP-cells, as well as respiration-deficient cells (RD-cells) and monocyte differentiated cells (D-cells). In this study [28], we obtained evidence for a stimulatory effect on the IP_3R, based on direct binding of the metalloid on upstream targets, which however caused the release of a limited amount of Ca^{2+}. This effect did not increase further at increasing concentrations of the metalloid, did not impair the Ca^{2+} response triggered by specific IP_3R agonists and was ROS-independent. We also found that IP_3R stimulation was associated with a very large Ca^{2+} release from the RyR. This effect was also ROS-independent and progressively increased at increasing arsenite concentrations. Furthermore, arsenite alone failed to release Ca^{2+} from the RyR, or to sensitize this channel to Ca^{2+}-induced Ca^{2+} release events triggered by the elevation of the cytosolic Ca^{2+} concentration ($[Ca^{2+}]_c$). Our interpretation of these findings was therefore that in addition to the direct stimulation of the IP_3R signaling, the metalloid also targets the IP_3R and RyR intraluminal crosstalk to increase significantly the release of Ca^{2+} through the second channel.

The present study addressed issues related to the regulation of mitochondrial Ca^{2+} uptake and accumulation, under the same conditions of arsenite exposure previously employed to investigate the effects of the metalloid on $[Ca^{2+}]_c$. More specifically, we asked questions related to the mechanism whereby Ca^{2+} is taken up by the mitochondria, as well as on the effects and consequences of this event in terms of ROS formation/regulation of both the survival and apoptotic signaling.

2. Materials and methods

2.1. Chemicals

Sodium arsenite, 2-aminoethoxydiphenyl borate (2-APB), Ry, AA, rotenone, caffeine (Cf), $CaCl_2$, ruthenium red (RR), $LaCl_3$, 7-chloro-5-(2-chlorophenyl)-1,5-dihydro-4,1-benzothiazepin-2(3H)-one (CGP-37157), Hoechst 33342, as well most of the reagent-grade chemicals were purchased from Sigma-Aldrich (Milan, Italy). Ru360 was obtained from Calbiochem (San Diego, CA). Cyclosporin A (CsA) was from Novartis (Bern, Switzerland). Fluo-4-acetoxymethyl ester, Rhod 2-acetoxymethyl ester, Dihydrorhodamine 123 (DHR), MitoSOX red, 10-N-nonyl acridine orange (NAO) and MitoTracker Red CMXRos were purchased from Molecular Probes (Leiden, The Netherlands).

2.2. Cell culture and treatment conditions

U937 human myeloid leukemia cells were cultured in suspension in RPMI 1640 medium (Sigma-Aldrich, Milan, Italy) supplemented with 10% fetal bovine serum (Euroclone, Celbio Biotecnologie, Milan, Italy), penicillin (100 units/ml) and streptomycin (100 μg/ml) (Euroclone), at 37 °C in T-75 tissue culture flasks (Corning Inc., Corning, NY, USA) gassed with an atmosphere of 95% air-5% CO_2. These cells were differentiated to monocytes by a 4 days growth in culture medium supplemented with 1.3% DMSO, as previous described [35]. U937 cells were made respiration-deficient as indicated in [25].

Sodium arsenite was prepared as a 1 mM stock solution in saline A (140 mM NaCl, 5 mM KCl, 4 mM $NaHCO_3$, and 5 mM glucose; pH 7.4) and stored at 4 °C. Cells (1.5×10^5 cells/ml) were exposed to arsenite in complete RPMI 1640 culture medium. Similar conditions were used in experiments employing permeabilized cells. Permeabilization was achieved by adding digitonin (10 μM) to a medium consisting of 0.25 M sucrose, 0.1% (w/v) BSA, 10 mM $MgCl_2$, 10 mM K^+-HEPES, and 5 mM KH_2PO_4 (pH 7.2) at 37 °C. Under these conditions, digitonin permeabilizes the plasma membrane but leaves mitochondrial membranes intact [36]. Treatments with AA were performed as detailed elsewhere [29].

2.3. Measurement of cytosolic and mitochondrial Ca^{2+} levels

The cells were supplemented with either 4 μM Fluo-4-acetoxymethyl ester or 10 μM Rhod 2-acetoxymethyl ester 30 min prior to the end of the treatments. After the treatments, the cells were washed three times and fluorescence images were captured with a BX-51 microscope (Olympus, Milan, Italy), equipped with a SPOT-RT camera unit (Diagnostic Instruments, Delta Sistemi, Rome, Italy) using an Olympus LCAch 40×/0.55 objective lens. The excitation and emission wavelengths were 488 and 515 nm (Fluo-4), and 540 and 590 nm (Rhod-2) with a 5-nm slit width for both emission and excitation. The light

intensity and the exposure settings were kept constant to allow quantitative comparisons of relative fluorescence intensity of cells between treatment groups. The exposure was limited to brief image acquisition intervals (≤ 5 s) to minimize photo-oxidation of Fluo-4 or Rhod-2. Fluorescence images (50 cells per sample from randomly selected fields) were digitally acquired and processed for fluorescence determination at the single cell level on a personal computer using the public domain Scion Image program. Briefly, single images were converted to 8-bit grayscale by linearly scaling from min-max to 0–255, where min and max are the two values displayed in the Image➢Adjust➢Brightness/Contrast. The obtained images were then inverted using the tool "Invert LUT". With inverted LUTs, pixels with a value of zero are white and pixels with a value 255 are black, the value (v) of each entry is replaced by 255-v. Mean fluorescence values were determined by averaging the fluorescence values of at least 50 cells/treatment condition/experiment.

2.4. DHR, MitoSOX red and NAO fluorescence assays

The cells were supplemented with either 10 μM DHR, 5 μM MitoSOX red or 10 μM NAO 30 min prior to the end of the treatments, washed three times with Saline A and subsequently analyzed with a fluorescence microscope. The resulting images were taken and processed as described above. The excitation and emission wavelengths were 488 and 515 nm (DHR), 510 and 580 nm (MitoSOX red), and 495 nm and 519 nm (NAO), with a 5-nm slit width for both emission and excitation. Mean fluorescence values were determined by averaging the fluorescence values of at least 50 cells/treatment condition/experiment.

2.5. Aconitase activity

The cells were washed twice with saline A, re-suspended in lysis buffer (50 mM Tris-HCl, 2 mM Na-citrate, 0.6 mM $MnCl_2$, pH 7.4) and finally sonicated three times on ice by using the Sonicator Ultrasonic Liquid Processor XL (Heat System-Ultrasonics, Inc., NY) operating at 20 W (10 s). The resulting homogenates were centrifuged for 5 min at $18{,}000 \times g$ at 4 °C. Aconitase activity was determined spectrophotometrically in the supernatants at 340 nm, as described in [37].

2.6. Measurement of DNA single-strand breakage by the alkaline halo assay

DNA single-strand breakage was determined using the alkaline halo assay developed in our laboratory [38]. It is important to note that, although we refer to DNA strand scission throughout the text, the DNA nicks measured by this technique under alkaline conditions may in fact include alkali labile sites in addition to direct strand breaks. Details on the alkaline halo assay and processing of fluorescence images and on the calculation of the experimental results are also given in Ref. [38]. DNA single-strand breakage was quantified by calculating the nuclear spreading factor value, representing the ratio between the area of the halo (obtained by subtracting the area of the nucleus from the total area, nucleus + halo) and that of the nucleus, from 50 to 75 randomly selected cells/experiment/treatment condition. Results are expressed as relative nuclear spreading factor values calculated by subtracting the nuclear spreading factor values of control cells from those of treated cells.

2.7. Western blot analysis

After treatments, the cells were processed to obtain the whole cell lysates as described in [39]. Equal amounts of proteins (25 μg) were resolved in 7% sodium dodecyl sulphate polyacrylamide gel and electrotransferred to polyvinyldiene difluoride membranes. Western blot analyses were performed using antibodies against Nrf2 (1:500, D1Z9C, Cell Signaling Technology, Leiden, The Netherlands) and actin (1:1000, sc-8432, Santa Cruz, Santa Cruz, CA). Details on Western blotting apparatus and conditions are reported elsewhere [40]. Antibody against actin were used to assess equal loading of the lanes.

2.8. Measurement of GSH content by high performance liquid chromatography

The cells (1×10^6) were suspended in 100 μl of lysis buffer (0.1% Triton X-100; 0.1 M Na_2HPO_4; 5 mM Na-EDTA, pH 7.5), vortexed and kept for 10 min on an ice bath. Thereafter, 15 μl of 0.1 N HCl and 140 μl of precipitating solution (0.2 M glacial meta-phosphoric acid, 5 mM sodium EDTA, 5 M NaCl) were added to the samples. After centrifugation, the supernatants were collected and kept at −20 °C until the HPLC analyses. Just before analysis, 60 μl of the acid extract were supplemented with 15 μl of 0.3 M Na_2HPO_4 and 15 μl of a solution containing 20 mg of DTNB in 100 ml of sodium citrate (1% w/v). The mixture was stirred for 1 min at room temperature and, after 5 min, filtered through 0.22 μm pore micro-filters. The resulting samples were finally analyzed for their GSH content by an HPLC assay [41], using a 15 cm × 4.6 mm, 5 μm Supelco Discovery® C18 column (Supelco, Bellefonte, PA). The UV absorption was detected at 330 nm. The injection volume was 20 μl. The retention time of GSH was approximately 15.7 min.

2.9. Measurement of mitochondrial membrane potential

The cells received 50 nM MitoTracker Red CMXRos 30 min prior to the end of the incubation with arsenite, were washed three times with Saline A and finally analyzed with a fluorescence microscope. The resulting images were taken and processed as described above. The excitation and emission wavelengths were 545 and 610 nm, respectively, with a 5-nm slit width for both emission and excitation. Mean fluorescence values were determined by averaging the fluorescence values of at least 50 cells/treatment condition/experiment.

2.10. Immunofluorescence analysis

After treatments, the cells were suspended in 2 ml of saline A and incubated for 30 min in 35-mm tissue culture dishes containing an uncoated coverslip. Under these conditions, cells rapidly attach to the coverslip. The cells were then fixed for 1 min with 95% ethanol/5% acetic acid, washed with phosphate buffer saline (PBS, 136 mM NaCl, 10 mM Na_2HPO_4, 1.5 mM KH_2PO_4, 3 mM KCl; pH 7.4) and blocked in PBS-containing bovine serum albumin (2% w/v) (30 min at room temperature). The cells were subsequently incubated with monoclonal anti-cytochrome c antibodies (1:100 in PBS containing 2% bovine serum albumin; Santa Cruz Biotechnology) stored for 18 h at 4 °C, washed and then incubated for 3 h in the dark with fluorescein isothiocyanate (Santa Cruz Biotechnology)-conjugated secondary antibody diluted 1:100 in PBS. The cells were then analyzed with a fluorescence microscope to count the relative numbers of cells bearing a punctate fluorescence, consistent with mitochondrial localization of cytochrome c, and a diffused fluorescence, consistent with the mitochondrial loss of cytochrome. In each experiment, at least 150 cells were analyzed to calculate the percentage of cells with a diffused fluorescence, indicative of MPT-dependent loss of cytochrome c.

2.11. Fluorogenic caspase 3 assay

Caspase 3-like activity was monitored as described in Guidarelli et al. [39] Briefly, the cells were lysed and aliquots of the extract (30 μg proteins) were incubated with 12 μM Ac-DEVD-AMC, at 30 °C. Caspase 3-like activity was determined fluorometrically (excitation at 360 nm and emission at 460 nm) by quantifying the release of aminomethylcoumarin (AMC) from cleaved caspase 3 substrate (Ac-DEVD-AMC).

2.12. Analysis of apoptosis with the Hoechst 33342 assay

After treatments, the cells were incubated for 5 min with 10 μM Hoechst 33342 and then analyzed with a fluorescence microscope to assess their nuclear morphology (chromatin condensation and fragmentation). Cells with homogeneously stained nuclei were considered viable.

2.13. Statistical analysis

The results are expressed as means ± SD. Statistical differences were analyzed by one-way ANOVA followed by Dunnett's test for multiple comparison or two-way ANOVA followed by Bonferroni's test for multiple comparison. A value of $P < 0.05$ was considered significant.

3. Results

3.1. Arsenite promotes mitochondrial Ca^{2+} accumulation

RP-cells were exposed for 6 h to 2.5 μM arsenite and subsequently processed for the assessment of both the $[Ca^{2+}]_c$ and $[Ca^{2+}]_m$, using respectively Fluo-4 and Rhod-2 as fluorescent probes. The results obtained in these experiments indicate that the metalloid promotes a significant increase in $[Ca^{2+}]_c$, as previously documented [28], as well as in the $[Ca^{2+}]_m$, as respectively shown in Supplementary Fig. 1A and B.

The results illustrated in Fig. 1A and B provide a quantification of the relative increases in the $[Ca^{2+}]_c$ and $[Ca^{2+}]_m$ and the additional information that both responses were suppressed by 2-APB, a IP_3R antagonist [42]. Fig. 1B also shows that the increase in $[Ca^{2+}]_m$ was suppressed by Ry, an antagonist of the RyR [19], and by Ru360, an inhibitor of mitochondrial Ca^{2+} uniporter (MCU) [43]. The increase in $[Ca^{2+}]_c$ (Fig. 1A) was instead significantly inhibited, but not suppressed, by Ry and insensitive to Ru360.

These results are indicative of a pivotal role of the RyR in processes leading to mitochondrial Ca^{2+} accumulation in cells exposed to arsenite. This notion is also consistent with the outcome of experiments showing that arsenite slightly elevates the $[Ca^{2+}]_c$ via 2-APB-sensitive and Ry- or Ru360- insensitive mechanisms in D-cells (Fig. 1A), which do not express the RyR. Under the same conditions, arsenite failed to increase the $[Ca^{2+}]_m$ (Fig. 1B).

The results presented in this section indicate that arsenite elevates the $[Ca^{2+}]_c$ and $[Ca^{2+}]_m$. It also appears that the fraction of the cation cleared by the mitochondria derives from the RyR and that mitochondrial Ca^{2+} uptake is mediated by a Ru360-sensitive mechanism. Some indication for the specificity of the effects of Ru360 is also provided by the absence of parallel effects on the $[Ca^{2+}]_c$.

3.2. Arsenite-induced mito$O_2^{\cdot-}$ formation is Ca^{2+}-dependent and requires mitochondrial Ca^{2+} accumulation

We recently demonstrated that the arsenite-induced Ca^{2+} mobilization from the IP_3R and RyR is not affected by mito$O_2^{\cdot-}$ released under the same conditions [28]. We therefore asked the question of whether the same is also true for events regulating mitochondrial Ca^{2+} uptake.

In order to address this question we used two different assays to measure ROS formation after a 6 h exposure of RP-cells to arsenite. We used DHR, a fluorescence probe allowing the detection of different radicals, including $O_2^{\cdot-}$, generated in both intra- and extra-mitochondrial compartments [44], and MitoSOX red, a fluorochrome commonly employed for the detection of $O_2^{\cdot-}$ in the mitochondria of live cells [45].

Arsenite promoted significant fluorescence responses using either of the two probes (Supplementary Fig. 1C and D). These different approaches also produced identical outcomes, in line with the notion that arsenite promotes mito$O_2^{\cdot-}$ formation, as we previously determined [24–27]. Both responses were indeed abolished by the complex I inhibitor rotenone, as well as by AA, supplemented under conditions promoting high and low concentrations of the vitamin in the mitochondria and cytosol, respectively (Fig. 1C and D) [29,30]. As indicated in Fig. 1B, these treatments however failed to affect the arsenite-induced increase in $[Ca^{2+}]_m$. Similar results were obtained by measuring the $[Ca^{2+}]_c$ (Fig. 1A) [28].

We also performed other experiments in RD-cells exposed for 6 h to 2.5 μM arsenite. These cells do not express a functional respiratory chain [25,26] and fail to respond to arsenite with increased mito$O_2^{\cdot-}$ formation (inset to Fig. 1C and D), but nevertheless accumulate Ca^{2+} in their cytosol (Fig. 1A) and mitochondria (Fig. 1B). These responses were identical to those observed in RP-cells and equally modulated by 2-APB, Ry and Ru360.

These results indicate that, in cells exposed to arsenite, the processes leading to Ca^{2+} mobilization and mitochondrial Ca^{2+} accumulation are ROS-independent.

We next investigated the role of Ca^{2+} in events leading to the formation of mito$O_2^{\cdot-}$ in cells exposed to arsenite. As illustrated in Fig. 1, the DHR- (C) and MitoSOX red (D) fluorescence responses detected in RP-cells exposed to the metalloid, besides being sensitive to rotenone or AA, were also suppressed by 2-APB, Ry or Ru360. The results illustrated in Table 1 indicate that the same treatments instead failed to affect the DHR-fluorescence response mediated by reagent H_2O_2, thereby providing evidence for the specificity of their protective effects.

These results are therefore consistent with the possibility that arsenite promotes mito$O_2^{\cdot-}$ formation via a Ca^{2+}-dependent mechanism, possibly regulated by the mitochondrial fraction of the cation. Consistent with this notion were the results from experiments using D-cells indicating the absence of mito$O_2^{\cdot-}$ formation (inset to Fig. 1C and D) in cells in which arsenite slightly increased the $[Ca^{2+}]_c$, via a 2-APB-sensitive/Ry-insensitive mechanism, but failed to increase the $[Ca^{2+}]_m$ (Fig. 1B).

We next used an alternative approach based on inhibition of mitochondrial Ca^{2+} efflux, an event expected to burst the arsenite-induced mito$O_2^{\cdot-}$ formation. For this purpose, we used CGP-37157, an inhibitor of mitochondrial Na^+/Ca^{2+} exchanger (mNCX) [46], and an exposure protocol (3 μM for 4 h) failing to produce detectable toxicity, as measured by either the trypan blue exclusion assay or the release of lactate dehydrogenase (not shown). An additional advantage of this exposure protocol is represented by the fact that, under these conditions, arsenite produces weak responses in terms of mitochondrial Ca^{2+} accumulation and mito$O_2^{\cdot-}$ formation (Table 2). We also found that CGP-37157 alone caused a weak increase in $[Ca^{2+}]_m$ in the absence of detectable effects on mito$O_2^{\cdot-}$ formation. It was then interesting to observe that combined exposure to arsenite and the mNCX inhibitor synergistically increased the $[Ca^{2+}]_m$ and mito$O_2^{\cdot-}$ formation.

In order to provide a final, direct evidence linking the mitochondrial fraction of Ca^{2+} to mito$O_2^{\cdot-}$ formation, we performed additional experiments using permeabilized RP-cells. In these experiments, the cells were first exposed to the appropriate fluorescence probe, subsequently permeabilized as detailed in the methods section, treated for 15 min with 2.5 μM arsenite, alone or with other additions, and finally analyzed for the $[Ca^{2+}]_m$ (Fig. 2A) and mito$O_2^{\cdot-}$ formation (Fig. 2B), as indicated above. Under these conditions, the metalloid failed to promote detectable effects, but nevertheless significantly enhanced mito$O_2^{\cdot-}$ formation when the $[Ca^{2+}]_m$ was increased via Cf supplementation. More specifically, we observed that Cf alone, or associated to arsenite, similarly increased the $[Ca^{2+}]_m$ and that the enhanced mito$O_2^{\cdot-}$ formation was only detected when the cells received both treatments. The increased $[Ca^{2+}]_m$ and mito$O_2^{\cdot-}$ formation were prevented by Ry, Ru360, RR (200 nM, a concentration specifically preventing mitochondrial Ca^{2+} uptake, [47]) and lanthanium ions ($LaCl_3$,100 μM, which competitively inhibits Ca^{2+} uptake, [48]). 2-APB failed to produce detectable effects under the same conditions.

We next performed experiments in which Cf was replaced with

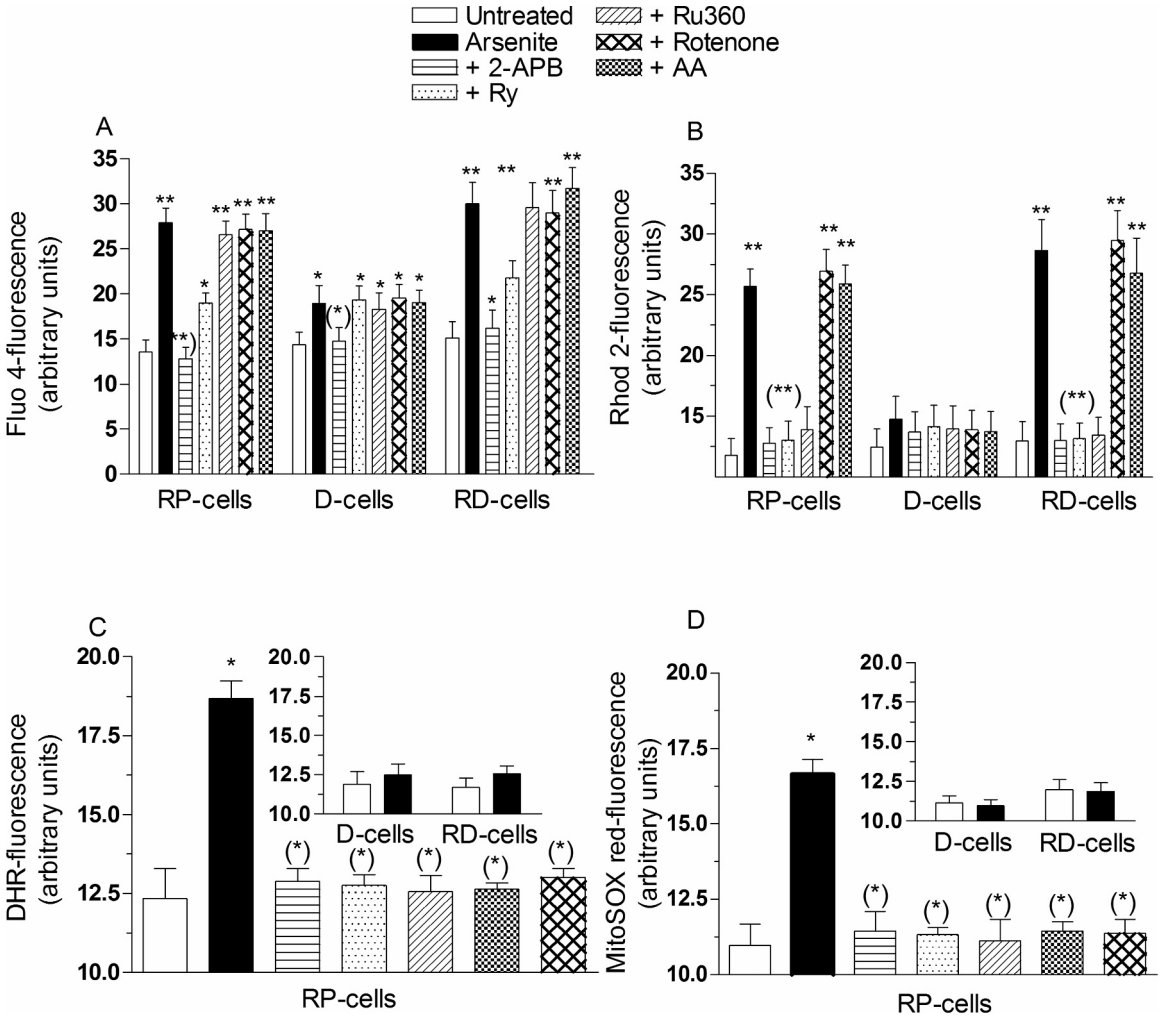

Fig. 1. Arsenite elevates the $[Ca^{2+}]_m$: the fraction of the cation cleared by the mitochondria derives from the RyR and critically mediates $mitoO_2^{\cdot-}$ formation. RP-, D- and RD-cells were pretreated for 15 min with 0 or 50 μM 2-APB, 20 μM Ry, 10 μM Ru360, 0.5 μM rotenone or 10 μM AA and incubated for 6 h with 2.5 μM arsenite. Cells were then loaded (30 min) with Fluo-4-AM (A) or Rhod-2-AM (B) and processed to determine their respective fluorescence responses. In other experiments, RP-cells were treated as indicated above, supplemented with DHR (C) or MitoSOX red (D) and analyzed for their respective fluorescence responses. The results obtained using D- and RD-cells are shown in the insets. Results represent the means ± SD calculated from 4 to 7 separate experiments. *P < 0.05, **P < 0.01, as compared to untreated cells. (*)P < 0.05, (**)P < 0.01, as compared to cells treated with arsenite (one-way ANOVA followed by Dunnet's test).

Table 1
Effect of various treatments on the DHR-fluorescence caused by H_2O_2.

Treatment	DHR-fluorescence (arbitrary units)
Untreated RP-cells	14.5 ± 1.4
H_2O_2	28.9 ± 2.5*
+ Rotenone	29.6 ± 2.2*
+ AA	27.4 ± 2.4*
+2-APB	30.1 ± 3.3*
+ Ry	27.7 ± 2.7*
+ Ru360	29.0 ± 2.6*

RP-cells were treated for 15 min with 0 or 50 μM H_2O_2, in the absence or presence of rotenone (0.5 μM), 2-APB (50 μM), Ry (20 μM) or Ru360 (10 μM). Drugs were added to the cultures 5 min prior to H_2O_2. AA (10 μM) was given to the cells 15 min prior to H_2O_2. After treatments, the cells were analyzed for DHR-fluorescence. Results represent the means ± SD calculated from at least 3 separate experiments.

* P < 0.001; as compared to untreated cells (one-way ANOVA followed by Dunnett's test).

reagent Ca^{2+} (30 μM), and observed a significantly increased mitochondrial Ca^{2+} accumulation (Fig. 2A) associated with enhanced $mitoO_2^{\cdot-}$ formation (Fig. 2B). Furthermore, both responses were sensitive to Ru360, RR and $LaCl_3$, but not to Ry, or 2-APB.

Table 2
CGP-37157 enhances the Rhod 2- or MitoSOX-red-fluorescence responses mediated by arsenite.

Treatment	Rhod 2-fluorescence (arbitrary units)	MitoSOX red-fluorescence (arbitrary units)
Untreated RP-cells	11.5 ± 1.4	11.3 ± 1.1
CGP-37157	16.9 ± 1.2	11.8 ± 1.3
Arsenite	20.4 ± 2.2	15.1 ± 1.5
Arsenite + CGP-37157	36.4 ± 2.4*	31.8 ± 2.6*

RP-cells were exposed for 4 h to arsenite (2.5 μM) in the absence or presence of CGP-37157 (3 μM). After treatments, the cells were analyzed for Rhod 2- or MitoSOX red-fluorescence. Results represent the means ± SD calculated from 3 separate experiments.

* P < 0.01, as compared to cells treated with arsenite (one-way ANOVA followed by Dunnett's test).

Collectively, the results presented in this section demonstrate that arsenite promotes mitochondrial Ca^{2+} accumulation via a mechanism insensitive to ROS. In addition, the experimental approach using both intact and permeabilized cells provided further indication for the specificity of the effects mediated by the different inhibitors and, most

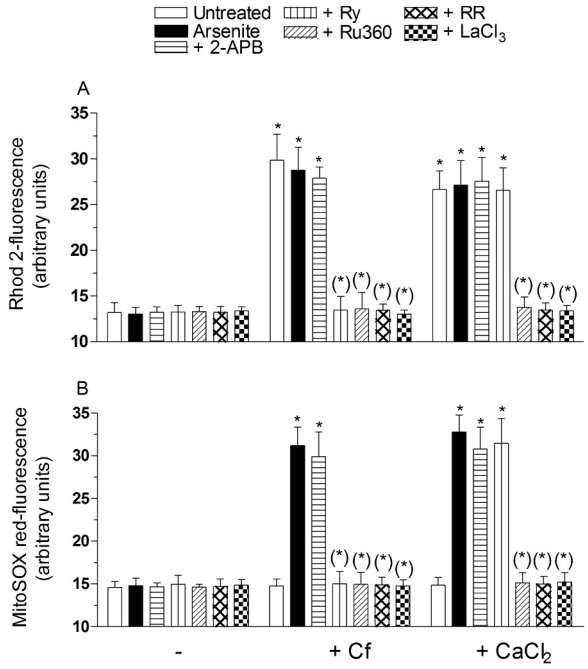

Fig. 2. The role of mitochondrial Ca^{2+} in events leading to mito$O_2^{\cdot-}$ formation: studies in permealized cells RP-cells were incubated for 20 min with Rhod-2-AM (A), re-suspended in digitonin buffer and finally exposed for 10 min to 2.5 μM arsenite, either alone or associated with 10 mM Cf, or 30 μM $CaCl_2$, in the absence or presence of 50 μM 2-APB, 20 μM Ry,10 μM Ru360, 200 nM RR or 100 μM $LaCl_3$. After treatments, the cells were analyzed for Rhod-2-fluorescence. In other experiments (B), intact RP-cells were initially incubated for 20 min with MitoSOX red, processed and treated as indicated in (A), and finally analyzed to determine the resulting fluorescence responses. Results represent the means ± SD calculated from 3 separate experiments. *P < 0.01, as compared to untreated cells. (*)P < 0.01, as compared to cells treated with arsenite (one-way ANOVA followed by Dunnet's test).

importantly, convincing experimental evidence causally linking the increased $[Ca^{2+}]_m$ with mito$O_2^{\cdot-}$ formation.

3.3. The increased mitochondrial Ca^{2+} concentrations are necessary to promote the indirect effects induced by arsenite on various biomolecules and on the Nrf2-dependent survival signaling

We previously determined that mito$O_2^{\cdot-}$-derived H_2O_2 mediates both the toxic and adaptive responses triggered by arsenite [27]. We can therefore predict that 2-APB, Ry and Ru360, by preventing mito$O_2^{\cdot-}$ formation (Fig. 1C and D), as previously observed with rotenone or AA [24,26,27], cause a parallel inhibition of the effects downstream to mito$O_2^{\cdot-}$ formation.

Indeed, as shown in Fig. 3, RP-cells exposed for 6 h to arsenite accumulated significant damage in their mitochondria in which we were able to detect decreased aconitase activity (A) and increased cardiolipin oxidation (B), using NAO as a fluorescent probe. Strand scission of genomic DNA, was also detected under the same conditions (C). In addition, we obtained evidence for increased Nrf2 expression (Fig. 3D) and GSH biosynthesis (Fig. 3E).

We found that all the above effects were prevented by 2-APB, Ry and Ru360. Arsenite instead failed to inhibit aconitase activity (A) and induce cardiolipin oxidation (B), DNA damage (C), Nrf2 expression (Fig. 3D) and GSH biosynthesis (Fig. 3E) in both D- and RD-cells, in which mito$O_2^{\cdot-}$formation did not take place (insets to Fig. 1C and D).

These results indicate that mitochondrial Ca^{2+} is critical for the arsenite-dependent induction of events associated with the formation of mito$O_2^{\cdot-}$ and hence with the ensuing damage in diverse biomolecules and activation of the Nrf2/GSH survival responses.

3.4. Transient vs sustained increase in $[Ca^{2+}]_c$ and $[Ca^{2+}]_m$

RP-cells were exposed for 6 h to 2.5 μM arsenite and incubated in fresh culture medium for additional 10 h prior to the assessment of the $[Ca^{2+}]_c$. The results illustrated in Fig. 4A indicate that the increase in $[Ca^{2+}]_c$ detected after 6 h was transient, and indeed the cytosolic Ca^{2+} signal measured after recovery was identical to that measured in untreated cells. Different results were instead obtained by measuring the Ca^{2+} response mediated by a 16 h exposure to the metalloid. We found that the $[Ca^{2+}]_c$ detected in these cells remained similar to that measured at the 6 h time-point.

The results obtained with RD-cells were identical to those described above for RP-cells, whereas the small increase in $[Ca^{2+}]_c$ detected in D-cells at 6 h disappeared after the post-treatment incubation and remained unchanged with the 16 h exposure regimen.

We subsequently found that the effects of the metalloid were also transient for the increased $[Ca^{2+}]_m$ (Fig. 4B). We were instead unable to measure the $[Ca^{2+}]_m$ in cells exposed for 16 h to arsenite, since under the same conditions a significant decline in mitochondrial membrane potential was also observed (Fig. 5A). Indeed Rhod 2, the probe employed in experiments measuring the $[Ca^{2+}]_m$, is taken up by the mitochondria as a function of their membrane potential [49].

It is however important to note that RD-cells, while failing to produced ROS in response to arsenite (Fig. 1C), were also resistant to the effects on mitochondrial membrane potential (Fig. 5A). In addition, a 6 h exposure of RD-cells to arsenite caused an increased $[Ca^{2+}]_m$ that returned to control levels after the 10 h post-incubation in fresh culture medium (Fig. 4B), as previously observed in RP-cells. RD-cells were therefore used to address the question of whether a sustained increase in $[Ca^{2+}]_m$ is observed after the 16 h exposure to arsenite. The results illustrated in Fig. 4B indicate that this was indeed the case. As expected, there was no evidence of mitochondrial Ca^{2+} accumulation in D-cells receiving any of the above treatments (Fig. 4B).

We subsequently moved to experiments measuring mito$O_2^{\cdot-}$ formation. As indicated in Fig. 4C, ROS formation in RP-cells exposed for 6 h to arsenite was suppressed by recovery in fresh culture medium, and significantly increased using the 16 h exposure paradigm (Fig. 4C). We also failed to detect increased mito$O_2^{\cdot-}$formation in D- or RD-cells receiving any of the above treatments (Fig. 4C).

We finally performed experiments measuring cardiolipin oxidation as an index of mitochondrial damage. As also previously indicated in Fig. 3B, a 6 h exposure to arsenite causes cardiolipin oxidation (Fig. 4D). This response was suppressed by recovery in fresh culture medium, and significantly increased using the 16 h exposure paradigm. In other words, the results obtained in these experiments were identical to those from experiments measuring mito$O_2^{\cdot-}$formation (Fig. 4C), which obviously makes sense since cardiolipin oxidation is mediated by mito$O_2^{\cdot-}$. As expected, there was no evidence of cardiolipin oxidation, in D- or RD-cells receiving any of the above treatments (Fig. 4D).

Collectively these results indicate that, under the conditions employed in the present study, the effects mediated by arsenite on the $[Ca^{2+}]_c$ and $[Ca^{2+}]_m$ are reversible upon post-treatment incubation of the cells in fresh culture medium. Evidence for mito$O_2^{\cdot-}$ formation was therefore restricted to cells exposed to arsenite without recovery. The 16 h exposure protocol instead promoted a sustained increase in both $[Ca^{2+}]_c$ and $[Ca^{2+}]_m$, associated with continuous and increasing mito$O_2^{\cdot-}$ formation.

3.5. Sustained increase in $[Ca^{2+}]_m$ is required to promote delayed toxic effects

As indicated above, and in our previous studies [24,26,27], inhibition of mitochondrial membrane potential is observed in RP-cells exposed for 16 h to arsenite (Fig. 5A). Furthermore, this event is associated with the mitochondrial loss of cytochrome c (Fig. 5B and Supplementary Fig. 1E), thereby confirming our previous findings

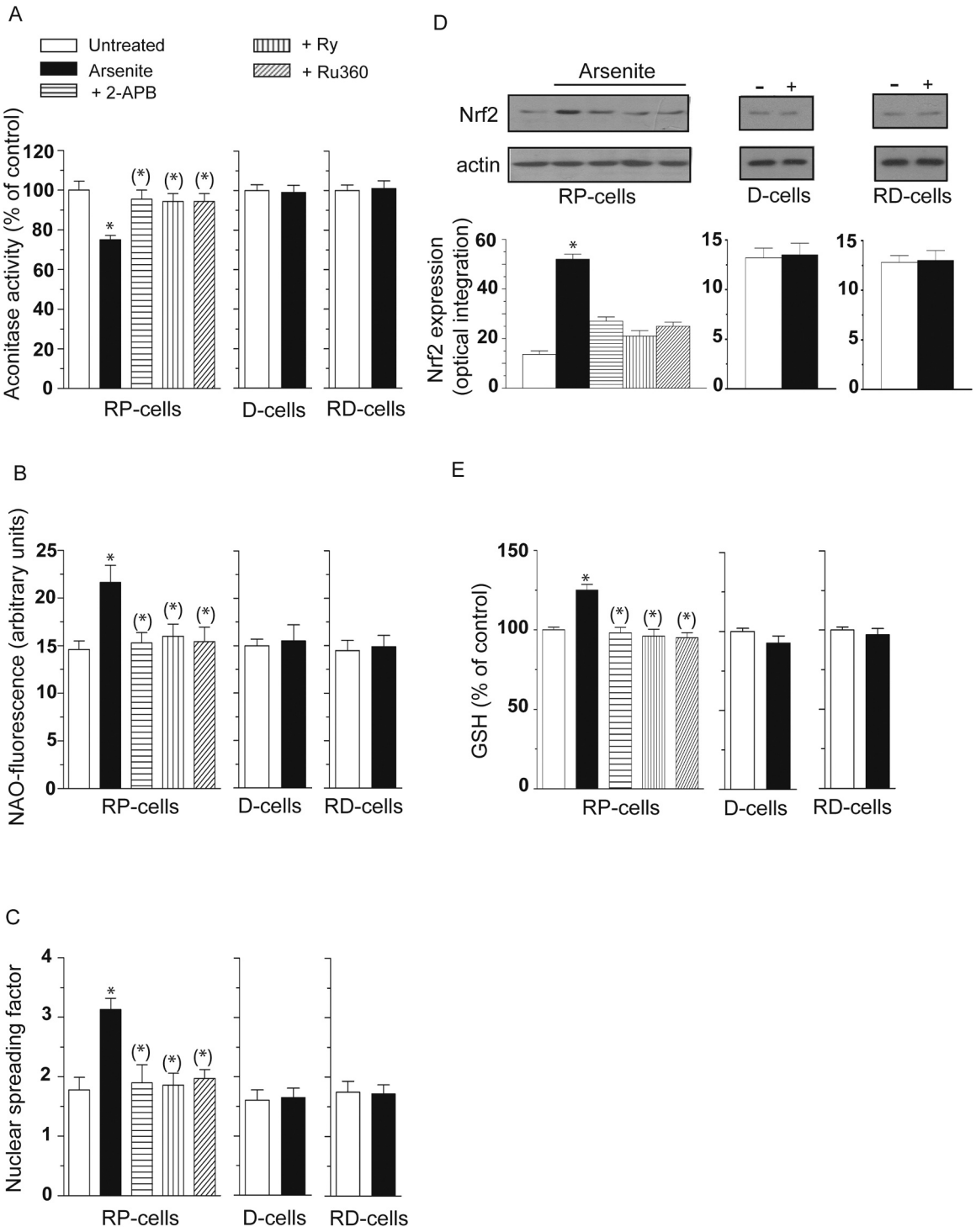

Fig. 3. Mitochondrial Ca^{2+} accumulation critically mediates the toxic effects induced by arsenite in mitochondrial and extramitochondrial compartments, as well as the parallel survival signaling. RP-, D- and RD-cells were exposed for 6 h to arsenite. RP cells also received the metalloid in the presence of 2-APB, Ry or Ru360. After treatments, the cells were analyzed for aconitase activity (A) NAO-fluorescence (B), DNA damage (C) and for their GSH content (E). In other experiments using identical conditions, except for the duration of arsenite exposure (4 h instead of 6 h), the cells were analyzed for Nrf2 expression (D). Blots shown in D (representative of three separate experiments) were re-probed for actin. Relative amounts of Nrf2 were quantified by densitometric analysis. Results represent the means ± SD calculated from 4 to 8 separate experiments. *P < 0.01, as compared to untreated cells. (*)P < 0.01, as compared to cells treated with arsenite (one-way ANOVA followed by Dunnet's test).

providing evidence for the induction of MPT [24,26,27]. This notion is in keeping with the observation that CsA (0.5 μM) prevents both events (not shown). These same events were also sensitive to treatments preventing the mitochondrial accumulation of Ca^{2+}. A longer exposure to arsenite (48 h) caused caspase 3 activation (Fig. 6A) and apoptotic DNA fragmentation (Fig. 6B). Both events were suppressed by CsA (not shown and [24,26,27]), 2-APB, Ry or Ru360.

We found no evidence for a decline in mitochondrial membrane potential (Fig. 5A), cytochrome c release (Fig. 5B), caspase 3 activation (Fig. 6A) and chromatin fragmentation (Fig. 6B) in RP-cells exposed for

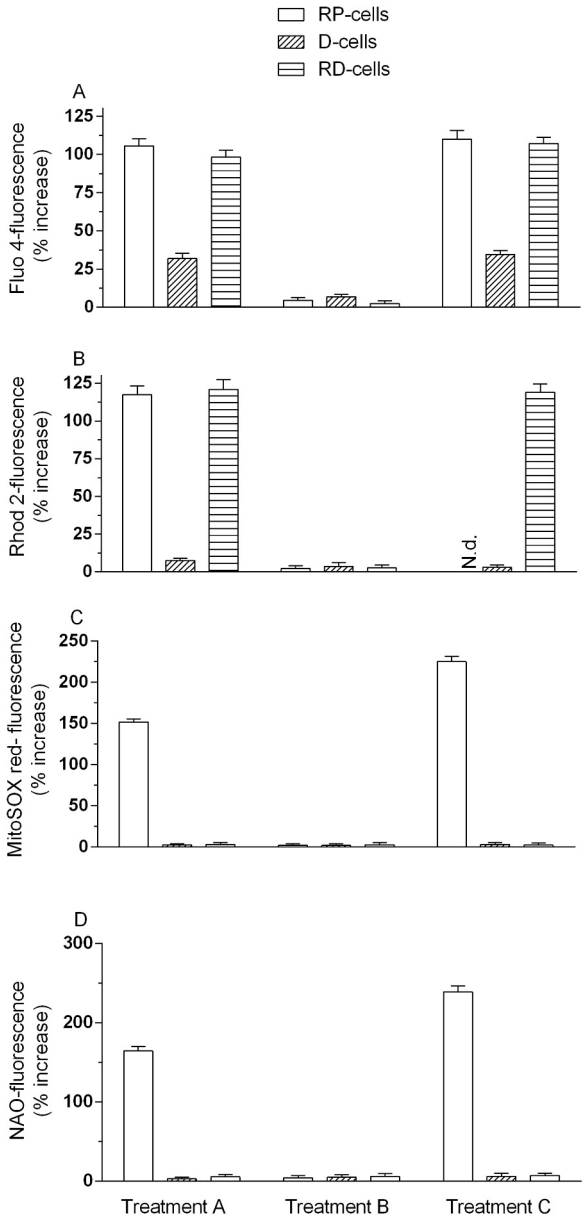

Fig. 4. The effects of arsenite on the $[Ca^{2+}]_c$ and $[Ca^{2+}]_m$ are reversible: prolonged exposure to the metalloid is required to promote a sustained increase of the concentration of the cation in mitochondria, necessary for mitochondrial dysfunction and apoptosis. RP-, D- and RD-cells were treated for 6 h with arsenite (Treatment A). Cells received Treatment A and were then incubated for a further 10 h in fresh culture (Treatment B). Cells were treated for 16 h with arsenite (Treatment C). After treatments, the cells were analyzed for Fluo- 4- (A), Rhod-2- (B), MitoSOX (C) or NAO- (D) fluorescence. Results represent the means ± SD calculated from 3 to 6 separate experiments.

6 h to arsenite, with or without recovery. As a final note, RD- and D-cells were resistant to mitochondrial dysfunction (Fig. 5A and B) and apoptosis (Fig. 6A and B) induced by prolonged arsenite exposure.

These results indicate that a sustained increase in $[Ca^{2+}]_c$ and, more specifically in $[Ca^{2+}]_m$, is critical for the induction of the arsenite-dependent delayed events. The 6 h exposure to the metalloid instead promotes reversible changes in both the $[Ca^{2+}]_c$ and $[Ca^{2+}]_m$. Exposure to arsenite followed by recovery in fresh culture medium was indeed associated with inhibition of mito$O_2^{\cdot-}$ formation, mitochondrial dysfunction and delayed apoptosis.

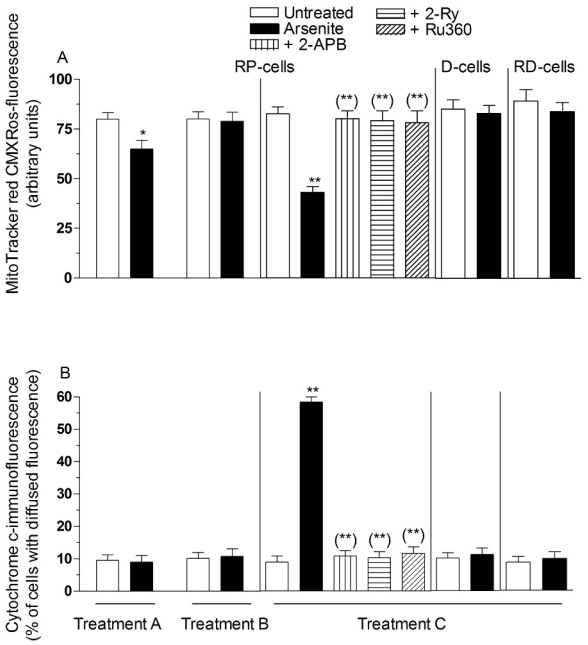

Fig. 5. Impact of transient *vs* sustained increase in the $[Ca^{2+}]_m$ on mitochondrial dysfunction. Cells were treated as indicated in the legend to Fig. 4, in which a definition of Treatment A-C is also provided. RP-cells received Treatment C also in the presence of 2-APB, Ry or Ru360. After treatments, the cells were analyzed for MitoTracker red CMXRos-fluorescence (A) and cytochrome c localization (B), as detailed in the Methods section. Results represent the means ± SD calculated from 4 to 6 separate experiments. *P < 0.05, **P < 0.01, as compared to untreated cells. (**)P < 0.01, as compared to cells treated with arsenite (one-way ANOVA followed by Dunnet's test).

4. Discussion

In a recent study, we investigated the effect of a low concentration of arsenite in a U937 cell line (RP-cells) and U937 cell variants with down-regulated RyR (D-cells) or characterized by a non-functional mitochondrial respiratory chain (RD-cells). These cells, along with use of specific inhibitors, allowed the identification of events leading to increased $[Ca^{2+}]_c$ through the sequential involvement of the IP_3R and RyR [28]. More specifically, we observed that arsenite promotes a weak stimulation of the IP_3R and a significant amplification of the overall Ca^{2+} response through the RyR, an event dependent on direct effects of the metalloid on the intraluminal crosstalk between the IP_3R and RyR.

Using the same approach, we now report that the effects of arsenite on the $[Ca^{2+}]_c$ are associated with a significant increase in $[Ca^{2+}]_m$, likely mediated by the MCU, a channel characterized by a high selectivity and conductance for Ca^{2+}, but a low apparent affinity for the cation [50,51]. Although the involvement of MCU in the mitochondrial transport of the cation appears consistent with the outcome of various experimental studies (see below), it should nevertheless be mentioned that mitochondria can also uptake the cation by additional channels as the Ca^{2+}/H^+ exchanger Letm1, the mitochondrial RyR1 and transient receptor canonical 3 [52].

Our preliminary observation was that the fraction of Ca^{2+} mobilized by arsenite from the IP_3R fails to promote a $[Ca^{2+}]_c$ sufficiently high to allow transport of the cation in the mitochondria. A more correct interpretation of these findings should however be based on the well-established subcellular heterogeneity of the Ca^{2+} concentrations resulting from exposure to different stimuli in different cells [11–13]. The different subcellular concentrations of the cation in selected microdomains can therefore explain the specificity of the corresponding

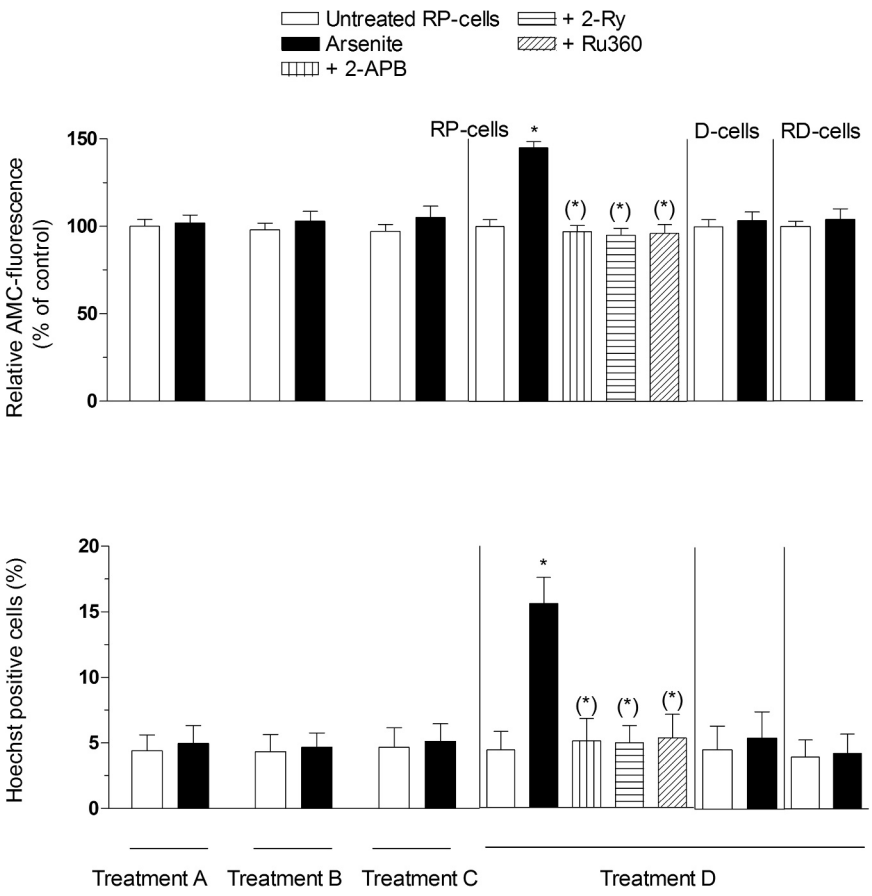

Fig. 6. Sustained increase in the $[Ca^{2+}]_m$ leads to apoptosis. Cells were treated as indicated in the legend to Fig. 4, in which a definition of Treatment A-C is also provided. Treatment D refers to cells exposed to the metalloid for 48 h. RP-cells received Treatment D also in the presence of 2-APB, Ry or Ru360. After treatments, the cells were analyzed for caspase-3 activity (A), or for apoptosis, by measuring chromatin fragmentation/condensation with the Hoechst assay (B). Results represent the means ± SD calculated from 5 separate experiments. *P < 0.01, as compared to untreated cells. (*)P < 0.01, as compared to cells treated with arsenite (one-way ANOVA followed by Dunnet's test).

functional effects [11,53,54]. Likewise, the possibility of Ca^{2+} transport in mitochondria is restricted to conditions in which the concentration of the cation is particularly high in the close proximity of the MCU [51,54]. These requirements therefore lead us to conclude that the Ca^{2+} released by the IP_3R in response to arsenite fails to create local concentrations of the cation permissive for transport through the MCU.

We subsequently determined that the fraction of Ca^{2+} released by the RyR after IP_3R stimulation induced by arsenite is instead efficiently cleared by the mitochondria. It therefore appears that the RyR-released Ca^{2+} promotes sufficient local concentrations of the cation in specialized microdomains created by the close association between mitochondria and the portion of the endoplasmic reticulum bearing the RyR channel. As a consequence, RyR-derived Ca^{2+} is readily transported by the MCU into mitochondria.

To summarize, the experimental results thus far discussed suggest that the direct effects of arsenite on the intraluminal IP_3R/RyR crosstalk identified in our previous work [28] are functional to RyR-dependent Ca^{2+} release coupled with MCU-dependent mitochondrial Ca^{2+} accumulation.

Having previously demonstrated that $mitoO_2^{\cdot-}$, and its dismutation product H_2O_2, produces hardly any effect on the arsenite-induced Ca^{2+} mobilization from the IP_3R and the RyR [28], we investigated whether the same was also true for events leading to enhanced mitochondrial Ca^{2+} accumulation. Our approach, based on the use of treatments preventing ROS formation, or RD-cells, univocally demonstrated that mitochondrial Ca^{2+} accumulation is also ROS-independent.

We subsequently investigated whether Ca^{2+} is necessary for ROS formation and found that treatments preventing the increase in $[Ca^{2+}]_c$ and $[Ca^{2+}]_m$ produce parallel inhibitory responses in terms of $mitoO_2$ formation in RP-cells. Furthermore, using RP-cells treated with Ry or D-cells, which do not express the RyR, we determined that the specific fraction of the cation involved in $mitoO_2^{\cdot-}$ formation is derived from the RyR. In other words, it appears that RyR-derived Ca^{2+} plays a critical role in the regulation of events associated with $mitoO_2^{\cdot-}$ formation. Since the fraction of Ca^{2+} taken up by the mitochondria also derives from the RyR, it would make sense to postulate its involvement in ROS formation. Our experiments performed in intact cells using Ru360 provided outcomes consistent with this conclusion. Indeed the MCU inhibitor, while failing to affect the $[Ca^{2+}]_c$, prevented the increase in $[Ca^{2+}]_m$ and caused a parallel suppression of $mitoO_2^{\cdot-}$ formation.

Consistently, inhibition of Ca^{2+} efflux from mitochondria mediated by CGP-37157 was associated with a dramatic increase in the arsenite-induced $mitoO_2^{\cdot-}$ formation.

Inhibitor studies, however, while validated by parallel observations ruling out the possibility of non-specific effects on Ca^{2+} homeostasis and/or on ROS formation, require converging information from studies using different approaches.

We therefore tried to establish a more direct link between mitochondrial Ca^{2+} accumulation and $mitoO_2^{\cdot-}$ formation using permeabilized cells, which allow the use of treatments that cannot be employed in intact cells. We preliminarily demonstrated that, under these conditions, Cf (a RyR agonist) promotes mitochondrial Ca^{2+} accumulation. The observation that such event can be clearly observed in permeabilized cells, implies the existence of a close proximity between the RyR and mitochondria of RP-cells. The same conclusion was reached in studies using arsenite, which also promotes Ca^{2+} release from this channel and causes mitochondrial Ca^{2+} accumulation. Regardless of this consideration, however, an important observation we could make was that even a short-term exposure to arsenite promotes $mitoO_2^{\cdot-}$ formation in cells manipulated to induce an enforced mitochondrial Ca^{2+} accumulation. In addition, as also observed in intact cells, the increase in $[Ca^{2+}]_m$ was necessary -but not sufficient- for ROS formation.

We also used a different approach in which reagent Ca^{2+} was

directly delivered to the permeabilized cells to then obtain results consistent with those described above, in which Cf was used to promote mitochondrial Ca^{2+} accumulation. As a final note, a further proof of concept documenting the involvement of mitochondrial Ca^{2+} in ROS formation is provided by experiments using Ru360, low concentrations of RR or an excess concentration of lanthanium ions. These different treatments effectively prevented both the mitochondrial Ca^{2+} accumulation and ROS formation stimulated by arsenite in the presence of either Cf or reagent Ca^{2+}.

Collectively, the above results provide solid experimental evidence supporting the notion that mitochondrial Ca^{2+} accumulation induced by arsenite is mediated by the MCU, ensues as a consequence of Ca^{2+} release form the RyR and critically mediates mito$O_2^{\cdot-}$ formation.

$O_2^{\cdot-}$ formation in different subcellular compartments generates different local concentrations of H_2O_2. For this reason, and for the compartmentalized nature of the antioxidant defenses [3,4], the indirect effects mediated by arsenite through the $O_2^{\cdot-}/H_2O_2$ signaling may vary significantly with different sites of $O_2^{\cdot-}$ formation. It follows that the effects mediated by arsenite in the specific paradigm employed in this study are profoundly affected by the ability of the metalloid to uniquely produce mito$O_2^{\cdot-}$ in U937 cells, which in turn appears to depend on mitochondrial Ca^{2+} accumulation consequent to the direct effects of the metalloid on the ER. Not surprisingly, prevention of mitochondrial Ca^{2+} accumulation was invariably associated with inhibition of the early effects mediated by arsenite through the intermediate formation of $O_2^{\cdot-}$ and H_2O_2 in mitochondrial (aconitase inhibition and cardiolipin oxidation) and extramitochondrial (strand scission of genomic DNA) compartments. Likewise, prevention of mitochondrial Ca^{2+} accumulation also abolished the cytoprotective signaling based on activation of the Nrf2 pathway leading to increased GSH biosynthesis.

Our previous work demonstrated that arsenite triggers two opposite events, both mediated by mito$O_2^{\cdot-}$ and H_2O_2 [27]. On the one hand, the oxidant(s) promoted the formation of lesions on vicinal and distal biomolecules, as indicated above (6 h), culminating in mitochondrial dysfunction and MPT (16 h) and followed by a delayed (48 h) apoptotic response [24,26,27]. On the other hand, $O_2^{\cdot-}$ and H_2O_2 also promoted a survival signaling based on activation of Nrf2, enhanced γ-glutamilcysteine synthase catalytic heavy subunit expression and increased GSH biosynthesis [27]. This latter event reduced the rate/extent of mito$O_2^{\cdot-}$ formation and, as a consequence, delayed and mitigated the extent of the above downstream deleterious effects.

We now provide details on the reasons why the above sequence of events requires the continuous presence of arsenite. Indeed, cells exposed for 6 h to the metalloid maintained intact and functional mitochondria, and remained viable when post-incubated in fresh culture medium since ROS formation ceased after the 10 h recovery, as a consequence of the inhibition of events causing deregulated Ca^{2+} homeostasis and increased mitochondrial Ca^{2+} accumulation. In addition, prevention of mitochondrial Ca^{2+} accumulation achieved with the use of various inhibitors, or D-cells, was invariably associated with the suppression of the toxic effects mediated by the metalloid. As previously noted, however, the increase in $[Ca^{2+}]_m$ is necessary but not sufficient to promote cytotoxicity, since the effects detected in RD-cells were identical to those measured in RP-cells in terms of variations in $[Ca^{2+}]_m$, but different in terms of mito$O_2^{\cdot-}$ formation and toxicity. Identical findings were obtained using RP-cells supplemented with agents preventing mito$O_2^{\cdot-}$ formation.

We therefore conclude that mitochondrial Ca^{2+} accumulation represents the *primum movens* of the effects of arsenite in the specific cell line employed, in which the metalloid only generates mito$O_2^{\cdot-}$. The source of the cation appears to be the RyR and its significant accumulation in mitochondria, while failing per se to produce direct consequences, was nevertheless critical for mito$O_2^{\cdot-}$ formation, the upstream species responsible for the cytoprotective and toxic effects mediated by the metalloid. These early events are however reversible and mito$O_2^{\cdot-}$ formation ceases when the $[Ca^{2+}]_m$ returns to normal levels. Sustained increase in $[Ca^{2+}]_m$ is therefore required for continuous ROS formation, and for the onset of MPT [24,26,27], thereby making necessary a more prolonged exposure to arsenite in order to obtain evidence of toxicity.

Acknowledgements

This work was supported by Ministero dell'Università e della Ricerca Scientifica e Tecnologica, Programmi di Ricerca Scientifica di Rilevante Interesse Nazionale, 2015, (Grant number: 2015MJBEM2-003. O.C.).

Author contribution

AG and OC conceived the research. AG, MF and LC performed the experiments. AG, MF, LC and OC analyzed the data. OC wrote the manuscript. AG, MF, LC and OC revised the manuscript. All authors approved the final version of the manuscript.

Conflict of interest statement

The authors have declared that they have no conflicts of interest.

Appendix A. Supporting information

Supplementary data associated with this article can be found in the online version at doi:10.1016/j.redox.2018.10.015

References

[1] K.M. Holmstrom, T. Finkel, Cellular mechanisms and physiological consequences of redox-dependent signalling, Nat. Rev. Mol. Cell. Biol. 15 (2014) 411–421.
[2] A.V. Kudryavtseva, G.S. Krasnov, A.A. Dmitriev, B.Y. Alekseev, O.L. Kardymon, A.F. Sadritdinova, M.S. Fedorova, A.V. Pokrovsky, N.V. Melnikova, A.D. Kaprin, A.A. Moskalev, A.V. Snezhkina, Mitochondrial dysfunction and oxidative stress in aging and cancer, Oncotarget 7 (2016) 44879–44905.
[3] H. Sies, C. Berndt, D.P. Jones, Oxidative stress, Annu. Rev. Biochem. 86 (2017) 715–748.
[4] D.E. Handy, J. Loscalzo, Redox regulation of mitochondrial function, Antioxid. Redox Signal. 16 (2012) 1323–1367.
[5] D.B. Zorov, M. Juhaszova, S.J. Sollott, Mitochondrial reactive oxygen species (ROS) and ROS-induced ROS release, Physiol. Rev. 94 (2014) 909–950.
[6] E. Bertero, C. Maack, Calcium signaling and reactive oxygen species in mitochondria, Circ. Res. 122 (2018) 1460–1478.
[7] S. Dikalov, Cross talk between mitochondria and NADPH oxidases, Free Radic. Biol. Med. 51 (2011) 1289–1301.
[8] E. Schulz, P. Wenzel, T. Munzel, A. Daiber, Mitochondrial redox signaling: interaction of mitochondrial reactive oxygen species with other sources of oxidative stress, Antioxid. Redox Signal. 20 (2014) 308–324.
[9] A. Gorlach, K. Bertram, S. Hudecova, O. Krizanova, Calcium and ROS: a mutual interplay, Redox Biol. 6 (2015) 260–271.
[10] A.L. Chernorudskiy, E. Zito, Regulation of calcium homeostasis by ER redox: a close-up of the ER/mitochondria connection, J. Mol. Biol. 429 (2017) 620–632.
[11] G. Csordas, D. Weaver, G. Hajnoczky, Endoplasmic reticular-mitochondrial contactology: structure and signaling functions, Trends Cell Biol. 28 (2018) 523–540.
[12] C. Hidalgo, P. Donoso, Crosstalk between calcium and redox signaling: from molecular mechanisms to health implications, Antioxid. Redox Signal. 10 (2008) 1275–1312.
[13] M. Trebak, R. Ginnan, H.A. Singer, D. Jourd'heuil, Interplay between calcium and reactive oxygen/nitrogen species: an essential paradigm for vascular smooth muscle signaling, Antioxid. Redox Signal. 12 (2010) 657–674.
[14] A. Guidarelli, C. Sciorati, E. Clementi, O. Cantoni, Peroxynitrite mobilizes calcium ions from ryanodine-sensitive stores, a process associated with the mitochondrial accumulation of the cation and the enforced formation of species mediating cleavage of genomic DNA, Free Radic. Biol. Med. 41 (2006) 154–164.
[15] M.B. Shakoor, R. Nawaz, F. Hussain, M. Raza, S. Ali, M. Rizwan, S.E. Oh, S. Ahmad, Human health implications, risk assessment and remediation of As-contaminated water: a critical review, Sci. Total Environ. 601–602 (2017) 756–769.
[16] B.C. Minatel, A.P. Sage, C. Anderson, R. Hubaux, E.A. Marshall, W.L. Lam, V.D. Martinez, Environmental arsenic exposure: from genetic susceptibility to pathogenesis, Environ. Int. 112 (2018) 183–197.
[17] S.J. Flora, Arsenic-induced oxidative stress and its reversibility, Free Radic. Biol. Med. 51 (2011) 257–281.
[18] S. Shen, X.F. Li, W.R. Cullen, M. Weinfeld, X.C. Le, Arsenic binding to proteins, Chem. Rev. 113 (2013) 7769–7792.
[19] G. Meissner, The structural basis of ryanodine receptor ion channel function, J. Gen.

Physiol. 149 (2017) 1065–1089.
[20] A. Chen, E.H. Cao, T.C. Zhang, J.F. Qin, Arsenite-induced reactive oxygen species and the repression of alpha-tocopherol in the MGC-803 cells, Eur. J. Pharmacol. 448 (2002) 11–18.
[21] C. Banerjee, R. Goswami, S. Datta, R. Rajagopal, S. Mazumder, Arsenic-induced alteration in intracellular calcium homeostasis induces head kidney macrophage apoptosis involving the activation of calpain-2 and ERK in Clarias batrachus, Toxicol. Appl. Pharmacol. 256 (2011) 44–51.
[22] T. Suriyo, P. Watcharasit, A. Thiantanawat, J. Satayavivad, Arsenite promotes apoptosis and dysfunction in microvascular endothelial cells via an alteration of intracellular calcium homeostasis, Toxicol. Vitr. 26 (2012) 386–395.
[23] V. Pachauri, A. Mehta, D. Mishra, S.J. Flora, Arsenic induced neuronal apoptosis in guinea pigs is Ca^{2+} dependent and abrogated by chelation therapy: role of voltage gated calcium channels, Neurotoxicology 35 (2013) 137–145.
[24] A. Guidarelli, S. Carloni, W. Balduini, M. Fiorani, O. Cantoni, Mitochondrial ascorbic acid prevents mitochondrial $O_2^{\cdot-}$ formation, an event critical for U937 cell apoptosis induced by arsenite through both autophagic-dependent and independent mechanisms, Biofactors 42 (2016) 190–200.
[25] A. Guidarelli, M. Fiorani, S. Carloni, L. Cerioni, W. Balduini, O. Cantoni, The study of the mechanism of arsenite toxicity in respiration-deficient cells reveals that NADPH oxidase-derived superoxide promotes the same downstream events mediated by mitochondrial superoxide in respiration-proficient cells, Toxicol. Appl. Pharmacol. 307 (2016) 35–44.
[26] A. Guidarelli, M. Fiorani, L. Cerioni, M. Scotti, O. Cantoni, Arsenite induces DNA damage via mitochondrial ROS and induction of mitochondrial permeability transition, Biofactors 43 (2017) 673–684.
[27] M. Fiorani, A. Guidarelli, V. Capellacci, L. Cerioni, R. Crinelli, O. Cantoni, The dual role of mitochondrial superoxide in arsenite toxicity: signaling at the boundary between apoptotic commitment and cytoprotection, Toxicol. Appl. Pharmacol. 345 (2018) 26–35.
[28] A.F. Guidarelli, M. Cantoni, O, Low concentrations of arsenite target the intraluminal inositol 1, 4, 5-trisphosphate receptor/ryanodine receptor crosstalk to significantly elevate intracellular Ca^{2+}, J. Pharmacol. Exp. Ther. 367 (2018) 184–193.
[29] M. Fiorani, C. Azzolini, L. Cerioni, M. Scotti, A. Guidarelli, C. Ciacci, O. Cantoni, The mitochondrial transporter of ascorbic acid functions with high affinity in the presence of low millimolar concentrations of sodium and in the absence of calcium and magnesium, Biochim. Biophys. Acta 2015 (1848) 1393–1401.
[30] O. Cantoni, A. Guidarelli, M. Fiorani, Mitochondrial uptake and accumulation of vitamin C: what can we learn from cell cultures studies? Antioxid. Redox Signal. 29 (2018) 1502–1515.
[31] C. Azzolini, M. Fiorani, L. Cerioni, A. Guidarelli, O. Cantoni, Sodium-dependent transport of ascorbic acid in U937 cell mitochondria, IUBMB Life 65 (2013) 149–153.
[32] T. Sugiyama, M. Yamamoto-Hino, A. Miyawaki, T. Furuichi, K. Mikoshiba, M. Hasegawa, Subtypes of inositol 1,4,5-trisphosphate receptor in human hematopoietic cell lines: dynamic aspects of their cell-type specific expression, FEBS Lett. 349 (1994) 191–196.
[33] E. Hosoi, C. Nishizaki, K.L. Gallagher, H.W. Wyre, Y. Matsuo, Y. Sei, Expression of the ryanodine receptor isoforms in immune cells, J. Immunol. 167 (2001) 4887–4894.
[34] A. Guidarelli, L. Cerioni, M. Fiorani, O. Cantoni, Differentiation-associated loss of ryanodine receptors: a strategy adopted by monocytes/macrophages to prevent the DNA single-strand breakage induced by peroxynitrite, J. Immunol. 183 (2009) 4449–4457.
[35] M. Scotti, M. Fiorani, A. Guidarelli, O. Cantoni, Differentiation of promonocytic U937 cells to monocytes is associated with reduced mitochondrial transport of ascorbic acid, Oxid. Med. Cell. Longev. 2018 (2018) 4194502.
[36] G. Fiskum, S.W. Craig, G.L. Decker, A.L. Lehninger, The cytoskeleton of digitonin-treated rat hepatocytes, Proc. Natl. Acad. Sci. USA 77 (1980) 3430–3434.
[37] P.R. Gardner, Aconitase: sensitive target and measure of superoxide, Methods Enzymol. 349 (2002) 9–23.
[38] O. Cantoni, A. Guidarelli, Indirect mechanisms of DNA strand scission by peroxynitrite, Methods Enzymol. 440 (2008) 111–120.
[39] A. Guidarelli, L. Cerioni, I. Tommasini, M. Fiorani, B. Brune, O. Cantoni, Role of Bcl-2 in the arachidonate-mediated survival signaling preventing mitochondrial permeability transition-dependent U937 cell necrosis induced by peroxynitrite, Free Radic. Biol. Med. 39 (2005) 1638–1649.
[40] O. Cantoni, I. Tommasini, L. Cerioni, The arachidonate-dependent survival signaling preventing toxicity in monocytes/macrophages exposed to peroxynitrite, Methods Enzymol. 441 (2008) 73–82.
[41] S. Brundu, L. Palma, G.G. Picceri, D. Ligi, C. Orlandi, L. Galluzzi, L. Chiarantini, A. Casabianca, G.F. Schiavano, M. Santi, F. Mannello, K. Green, M. Smietana, M. Magnani, A. Fraternale, Glutathione depletion is linked with Th2 polarization in mice with a retrovirus-induced immunodeficiency syndrome, murine AIDS: role of proglutathione molecules as immunotherapeutics, J. Virol. 90 (2016) 7118–7130.
[42] T. Maruyama, T. Kanaji, S. Nakade, T. Kanno, K. Mikoshiba, 2APB, 2-aminoethoxydiphenyl borate, a membrane-penetrable modulator of Ins(1,4,5)P_3-induced Ca^{2+} release, J. Biochem. 122 (1997) 498–505.
[43] C. Zazueta, M.E. Sosa-Torres, F. Correa, A. Garza-Ortiz, Inhibitory properties of ruthenium amine complexes on mitochondrial calcium uptake, J. Bioenerg. Biomembr. 31 (1999) 551–557.
[44] A. Gomes, E. Fernandes, J.L. Lima, Fluorescence probes used for detection of reactive oxygen species, J. Biochem. Biophys. Methods 65 (2005) 45–80.
[45] P. Mukhopadhyay, M. Rajesh, G. Hasko, B.J. Hawkins, M. Madesh, P. Pacher, Simultaneous detection of apoptosis and mitochondrial superoxide production in live cells by flow cytometry and confocal microscopy, Nat. Protoc. 2 (2007) 2295–2301.
[46] M. Chiesi, R. Schwaller, K. Eichenberger, Structural dependency of the inhibitory action of benzodiazepines and related compounds on the mitochondrial Na^+-Ca^{2+} exchanger, Biochem. Pharmacol. 37 (1988) 4399–4403.
[47] E. Carafoli, Intracellular calcium homeostasis, Annu. Rev. Biochem. 56 (1987) 395–433.
[48] C.E. Thomas, D.J. Reed, Effect of extracellular Ca^{++} omission on isolated hepatocytes. II. Loss of mitochondrial membrane potential and protection by inhibitors of uniport Ca^{++} transduction, J. Pharmacol. Exp. Ther. 245 (1988) 501–507.
[49] A. Minta, J.P. Kao, R.Y. Tsien, Fluorescent indicators for cytosolic calcium based on rhodamine and fluorescein chromophores, J. Biol. Chem. 264 (1989) 8171–8178.
[50] Y. Kirichok, G. Krapivinsky, D.E. Clapham, The mitochondrial calcium uniporter is a highly selective ion channel, Nature 427 (2004) 360–364.
[51] E. Penna, J. Espino, D. De Stefani, R. Rizzuto, The MCU complex in cell death, Cell Calcium 69 (2018) 73–80.
[52] J. Mishra, B.S. Jhun, S. Hurst, O.U. J, G. Csordas, S.S. Sheu, The Mitochondrial Ca^{2+} uniporter: structure, function, and pharmacology, Handb. Exp. Pharmacol. 240 (2017) 129–156.
[53] R. Rizzuto, T. Pozzan, Microdomains of intracellular Ca2+: molecular determinants and functional consequences, Physiol. Rev. 86 (2006) 369–408.
[54] D. De Stefani, R. Rizzuto, T. Pozzan, Enjoy the trip: calcium in mitochondria back and forth, Annu. Rev. Biochem. 85 (2016) 161–192.